J. Micromech. Microeng. **18** (2008) 045020 (12pp) doi:10.1088/0960-1317/18/4/045020

Inter-substrate microstructure formation by electroplating bonding technology

Yeun-Ho Joung and Mark G Allen

School of Electrical and Computer Engineering, Georgia Institute of Technology, 791 Atlantic Drive Atlanta, GA 30332, USA

E-mail: yeunho@gmail.com

Received 16 October 2007, in final form 23 December 2007
Published 11 March 2008
Online at stacks.iop.org/JMM/18/045020

Abstract

This paper explores the technological capabilities as well as theoretical limitations of electroplating bonding technology (EBT). EBT is of particular interest for the fabrication of complex three-dimensional electrical components (e.g. inductors, high frequency antennae, etc) as well as high aspect ratio mechanical structures with exotic geometrical features. Two separate substrates, each containing identical arrays of 150 μm tall copper microstructures, are aligned and then joined together using electrodeposition of copper under forced convection conditions to form 300 μm long structures that mechanically and electrically link the two substrates. Theoretical and experimental approaches are used to develop this bonding system. Mass transfer calculations of diffusion and convection are performed to predict optimal fabrication conditions. To demonstrate the ability to predict optimal plating conditions, a test coupon mimicking a chip-scaled interconnect system with 256 chip interconnects is designed, fabricated and characterized. The mechanical and electrical connectivity are verified by formation of daisy-chained test beds. The electrical testing of the bonded system shows an excellent conductivity of 0.097 Ohm/test row. Thermal-cycling-accelerated aging tests are performed over a temperature range from −55 to +125 °C. Electroplating bonded structures show excellent mechanical stability as well as electrical performance.

(Some figures in this article are in colour only in the electronic version)

1. Introduction

Solutions for packaging in a microelectromechanical system (MEMS) are often optimized to attain specific goals: sheltering the microstructure from the external environment; improving its lifetime by minimizing extremes of temperature, moisture, dust and physical contact; or providing adequate electrical interconnectivity. Recently, many researchers have investigated methods to form the interconnection between a MEMS structure and a chip or another substrate [1–3]. To serve as signal or power lines for MEMS systems, the interconnect structures must be mechanically robust and exhibit good electrical conductivity in order to operate properly when subject to severe mechanical vibration, high temperature and high power density or to reliably transfer electrical signals. Moreover, manufacturability of the interconnects must be considered because 3D structured MEMS systems usually require fabrication sequences that are more complex than the conventional one.

Wire bonding, tape-automated bonding and flip-chip bonding are a few examples of currently used interconnection methods. Flip-chip bonding is often employed due to its ease of implementation, its efficient use of real estate and its short electrical line [4–6]. However, flip-chip reliability is difficult to achieve if the substrates being connected exhibit large differences in their thermal expansion properties. This often results in shortened lifetimes of the complete packaged systems.

An alternative method for packaging is introduced in this paper. We have developed a technique of using electrodeposition to electrically and mechanically join conductive structures on two separate substrates that are accurately brought into close proximity to each other. This is called 'electroplating bonding'. With this technology, we demonstrate the interconnection between a simulated chip and a packaging substrate. There are several motivations for developing this technology. First, electronic devices need to function over a specified range of temperature during their operation. Interconnect systems composed of materials having different properties of thermal expansion may exhibit reduced reliability due to thermally induced stresses. In the 1990s, researchers demonstrated a wire interconnect method [7] with Cu posts and solder bonding to improve the weakness of the solder joining, but this still has the potential problem of failure due to thermally induced stresses between the copper and the solder. Interconnects made using electroplating bonding technology (EBT) would not exhibit reduced reliability due to thermally induced stresses because the interconnects and the material used to join them are the same. Second, the electroplating bonding method can allow for the incorporation of additional devices in the gap between the two substrates [8]. This can lead to increased packaging density and improved electrical performance of the packaged system. Third, the technology has been demonstrated as a method of transferring structures between different substrates [8, 9].

In this paper, we present theoretical and experimental approaches for electroplating bonding technology. The theoretical approach is performed with mass transfer theory which is developed for a system exhibiting diffusion and convection. The diffusion and convection conditions, necessary to bond a chip of a certain size to a substrate, are estimated with the solutions of these equations for the various geometries of the experimental systems. These systems are then fabricated and tested in order to verify their electrical and mechanical characteristics. Simple electrical characterization is carried out by measuring the electrical resistance of the interconnections between conductive structures on both a chip and a flat substrate that are formed using electroplating bonding [10]. To assure thermal functionality of the electroplating bonded interconnect system, thermal reliability is also tested using a thermal cycle chamber.

2. General fabrication procedure for electroplating bonding

2.1. Electroplating bonding

Electroplating bonding is an application of electrodeposition for the purpose of making connections or contacts between two microstructures. The connections, built using this electroplating bonding process, can be applied to create interconnections or microstructures [8] between substrates. The fabrication concept of the technology can be explained as follows. Two substrates bearing metallic structures to be connected are brought together as in the flip-chip method. When this combination is then submerged in a plating solution and an electric potential is applied to the structures, an electroplated metal layer grows between the two separate structures on the two separate substrates, thus bonding them and forming a connection. A variety of metallic-electroplating solutions are available for electroplating bonding, including Cu, Au, Ni, Ni/Fe and other metals.

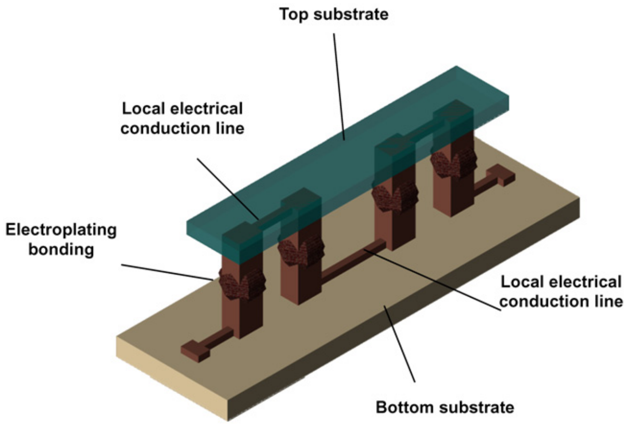

Figure 1. Schematic of the electrical conduction line of an electroplating bonding test coupon.

2.2. Design scheme of test coupons

The electrical conduction line is configured as shown in figure 1. Local electrical connections between two metal posts on both substrates form the electrical bridges, and the electrical paths between the bottom posts and top posts are accomplished by electroplating bonding. There are two purposes of inserting an electrical test bed into an electroplating bonding system: (1) verification of the integrity of mechanical connection of the bonded structures and (2) acquisition of approximate electrical resistance values of each bonded post. A test row for a daisy chain of 16 plating bonded metal posts is designed. If a post in the electrical test bed has a failure, then all posts exposed on the electroplating bonding process in the electrical test row are considered as failed posts in electroplating bonding. Two substrates are used to bond the posts. A substrate, hereafter to be called the bottom substrate, has the electrical contact pads. A glass as a top substrate is used for alignment purposes. The gap between the two substrates is 300 μm and the distance between the edge of the top substrate and the center of that substrate is over 15 000 μm. Therefore, the aspect ratio of this system is over 50:1.

2.3. General fabrication scheme

Samples are prepared with $16 \times 16 = 256$ Cu posts, with 150 μm height and 400 μm pitch, in an area of 1 cm $\times$ 1 cm on both substrates which contain the electrical conductive connection lines. The structures are fabricated using the process as described in figure 2. First, a Ti/Cu/Ti (300/2000/300 Å) seed layer is sputtered on both substrates to serve electrical current feedthrough for subsequent electroplating steps. The Cu electrical conduction line is then formed using a 20 μm thick layer of AZ 4620 photoresist mold and electroplating on both substrates. The Cu posts that are to be the electrical and mechanical interconnections between bottom and top substrates are fabricated using a layer of 150 μm high SU-8 epoxy negative photoresist and electroplating on both substrates. Then, the seed layer on the top substrate is etched away for aligning purposes and the seed layer on the bottom

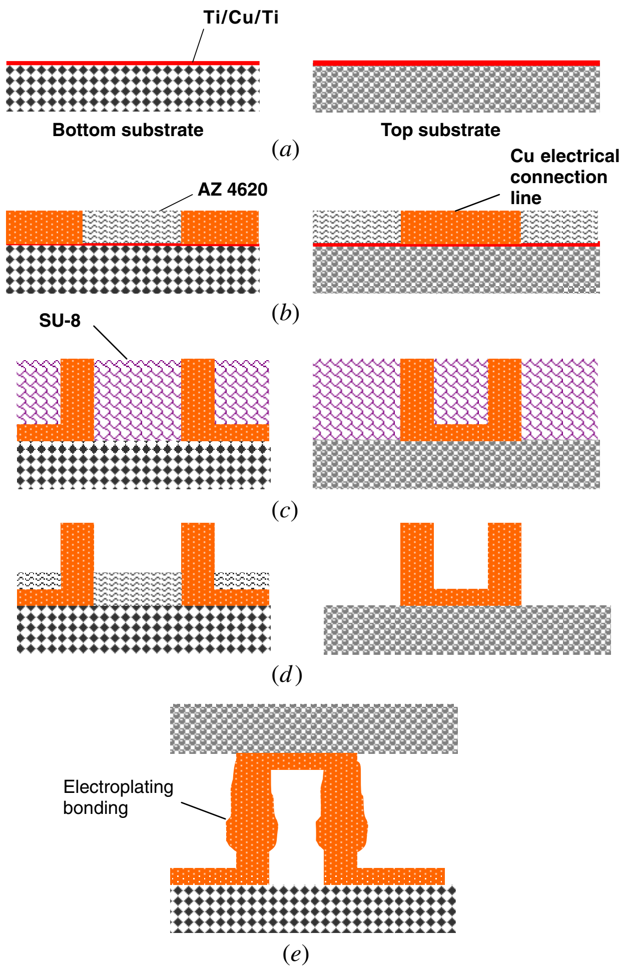

Figure 2. Fabrication procedure of electroplating bonding. (*a*) Seed deposition, (*b*) Cu electrical conduction line formation, (*c*) post-formation, (*d*) SU-8 etching and PR covering and (*e*) electroplating bonding.

substrate is covered by the AZ 4620 photoresist (except for the Cu post). Top and bottom structures are aligned, clamped and placed into an electroplating bath. Usually, the clamping gives less than a 15 μm gap between the posts. Seed layer removal occurs after the bonding sequence. This is accomplished by a removal of the polymer layer with a solvent followed by etching of the thin layers of Ti and Cu. The thickness of this Cu layer is much less than the thickness of the plated Cu. Therefore, the bonding quality of the Cu posts is not compromised. After electroplating bonding of the system, simple electrical and mechanical tests are performed. First, as a simple mechanical test, a nitrogen flow gun at the pressure of approximately 25 psi is used to test the mechanical integrity of the sample during the drying step of the fabrication scheme. The flow of nitrogen is directed at the gap between the substrates and applied for a duration of approximately 15 s. This is repeated for a total of ten times. If the system could survive sustained high-pressure nitrogen directed at the gap, then the electrical connection is tested using a standard multimeter.

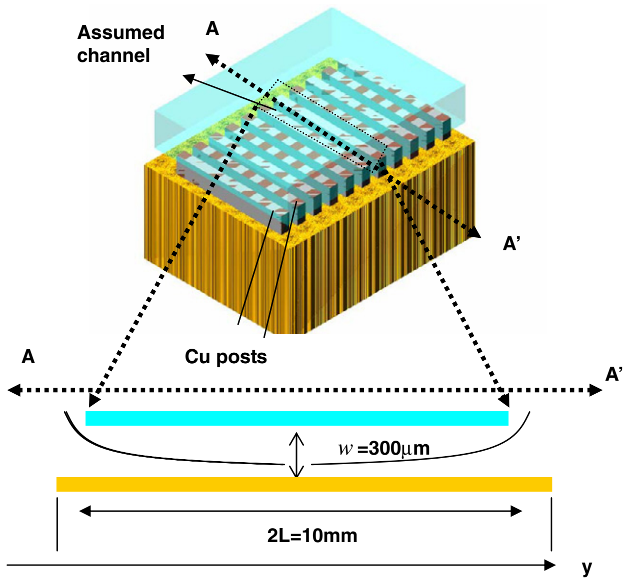

Figure 3. Schematic of a mass transfer system for a diffusion model (no convection).

3. Electroplating bonding with diffusion

3.1. Theoretical approach with a diffusion system

The mechanism of electrodeposition of Cu ions in this electroplating bonding system can be expressed by mass transfer theory, especially the influence of the diffusion effect in the non-convective electroplating bonding system. For Cu interconnections or plated-through-hole interconnections, Cu growth on the surface or at the entrance of the mold is faster than in the depth of the hole [11–13]. This phenomenon causes a more serious problem in a high aspect ratio (over 10:1) situation such as the diffusional electroplating bonding system. In order to simplify the analysis of the non-uniform Cu growth in the high aspect ratio electroplating bonding environment, it is initially assumed that the electrodeposition is totally dependent on the diffusion of Cu ions. At the beginning of electroplating, the Cu ions existing in the channel could be electrodeposited on the structure. However, after the initial current (i_0) is applied to the system, the Cu ion concentration is gradually depleted. Upon depletion of the Cu ions, fresh Cu ions must be transported to the deposition site. This rate of transport affects the deposition rate. If we assume that there is no convection effect inside of the gap, this transport is entirely due to diffusion. It is further assumed that the concentration of the bulk solution outside the gap is not variable at any time, and that the geometrical nonlinearity of the Cu posts has a minor influence on the analysis. Under these conditions, a theory can be developed for predicting the effect of ion depletion. For the purpose of analysis, it is assumed that the bonded posts produce a channel as described in figure 3(*a*). The symmetry of the diffusion distribution gives the possibility of additional simplification of the model geometry. Shell balance theory and symmetry of the diffusion distribution in the channel give that the half-length (L) of the channel can be considered in a one-dimensional model. By Fick's Law [14–16], the mass flux (J_i) is related to the gradient of Cu ion concentration of a stagnant solution in the high aspect ratio gap:

$$J_i(y) = -D_i \frac{dC_i(y)}{dy}, \tag{1}$$

where D_i is the Cu ion diffusivity in the Cu electroplating solution and C_i is the concentration of the interested ion. A typical value of D_i for the Cu ion in aqueous solutions is 5×10^{-6} cm^2 s^{-1} [14]. Other references give slightly higher values. In this work, D_i is assumed as 5.5×10^{-6} cm^2 s^{-1}. By conservation of mass,

$$\frac{dJ_i(y)}{dy} = -D_i \frac{d^2C_i(y)}{dy^2} = 0. \tag{2}$$

The relation between replenishment of Cu ion by diffusion and consumption of Cu ion by electrodeposition in the channel can expressed as

$$D_i \frac{d^2C_i(y)}{dy^2} = \frac{a_s i_i(C)}{nF}, \tag{3}$$

where F is Faraday's constant (F) (9.648 99 $\times 10^4$ C gmol^{-1}), i_i is the current changed by concentration of the interested ion, n is the number of transferred electrons due to copper reduction, a_s is the specific surface area ($2/w$) (area/volume) and w is the channel height [17]. If we only consider the effect of concentration on current (i_i) and assume that the total number of electrons transferred to the electrode in a unit time must be proportional to the quantity of electroactive substance reaching the electrode in that time period [14], then i_i can be expressed as

$$i_i = i_0 \frac{C_i(y)}{C_0}, \tag{4}$$

where i_0 is a initial current and C_0 is a concentration of the interested ion at $y = 0$.

Then,

$$D_i \frac{d^2C_i(y)}{dy^2} = \frac{2i_0}{wnFC_0} C_i(y). \tag{5}$$

To solve equation (5), first consider a nondimensionalization given by $C^* = C_i(y)/C_0$ and $y^* = y/L$. Then equation (5) can be written as

$$\frac{d^2C_i^*(y^*)}{dy^{*2}} - \xi_D C_i^*(y^*) = 0, \tag{6}$$

where ξ_D is a nondimensional diffusion parameter given by

$$\xi_D = \frac{2i_0L^2}{DwnFC_0}. \tag{7}$$

The magnitude of the diffusion parameter (7) determines the relative importance of diffusional resistance to the copper ion transport as will be discussed in more detail below. Appropriate boundary conditions for the solution of equation (6) are $C_i^* = 1$ at $y* = 0$ (i.e. the concentration of Cu ion is equal to the bulk concentration at the entrance to the channel) and $dC_i/dy^* = 0$ at $y* = 1$ (i.e. the Cu ion concentration is symmetric with regards to the entire channel length). Equation (6) can be solved as a homogeneous second-order linear differential equation with real constant coefficients. The associated characteristic equation of equation (6) is $\lambda^2 - d^2\lambda = 0$, where $d = (\xi_D)^{1/2}$. Then,

$$C_i^* = \frac{e^{d \cdot y^*} + e^{d(2-y^*)}}{1 + e^{2d}}. \tag{8}$$

The physical meaning of ξ_D can be explained with the exact solution of equation (6). This dimensionless parameter quantifies the relative importance of diffusional resistance relative to the consumption of Cu ion. As shown in figure 4(*a*), values of $\xi_D > 1$ indicate that diffusional resistance is important and the Cu ion is substantially depleted inside the trench or channel. For $\xi_D \ll 1$, diffusional resistance is small, so Cu ions are not significantly depleted inside the feature. It is instructive to create a predictive model for the electroplating bonding system using the diffusion equation. Several numerical analyses are performed with a designated system that has a predetermined value such as channel lengths (5 mm) drawn from realistic chip die sizes and constants such as Faraday's constant (F), Cu ion diffusivity and the number of transferred electrons due to copper reduction. An initial analysis is performed as a function of the current with fixed concentration of Cu ions (1 M or 0.001 g mol cm^{-3}), which is the concentration of the copper plating solution during electroplating bonding, and a 300 μm channel height which is taken as a realistic value for electroplating bonding fabrication of the interconnect system. For the analysis, 0.01, 0.05, 0.1, 2.5 and 10 mA cm^{-2} current densities are applied to the equation. Substitution of these parameters (except for the varying current density) into equation (6) yields

$$\xi_D = 15.7 i_0, \tag{9}$$

where i_0 is in mA cm^{-2}. Figure 4(*b*) shows the concentration variation versus channel distance as a function of current density. The diffusion length decreases as the current density increases. However, too small of a value is not applicable because plating time is increased as current is decreased. It is clear from figure 4(*b*) that no realistic current density value will solve the depletion problem for typical electroplating bonding geometries of interest. Next, the effect of channel height is examined. In this analysis, 10 mA cm^{-2} which is used in a real electroplating bonding system is chosen for the current density. The applicable height variables are 200, 300, 400, 500 and 600 μm. Heights larger than these values are not considered because interconnect that is too high has the possibility of inducing high electrical parasitics, and can also produce mechanically unstable structures. Because higher aspect ratio systems will only make the diffusion limitation worse, i.e. increase the diffusion parameter, heights under 200 μm are not considered. Substitution of these parameters (except for the varying height) into equation (6) yields

$$\xi_D = \frac{4.71}{w}, \tag{10}$$

where w is in centimeters. Figure 4(*c*) shows the concentration variation versus distance from the mouth of the channel as a function of channel height. The analysis proves that the diffusion parameter value with high channel geometry is less than that of a low channel system, as expected. Moreover,

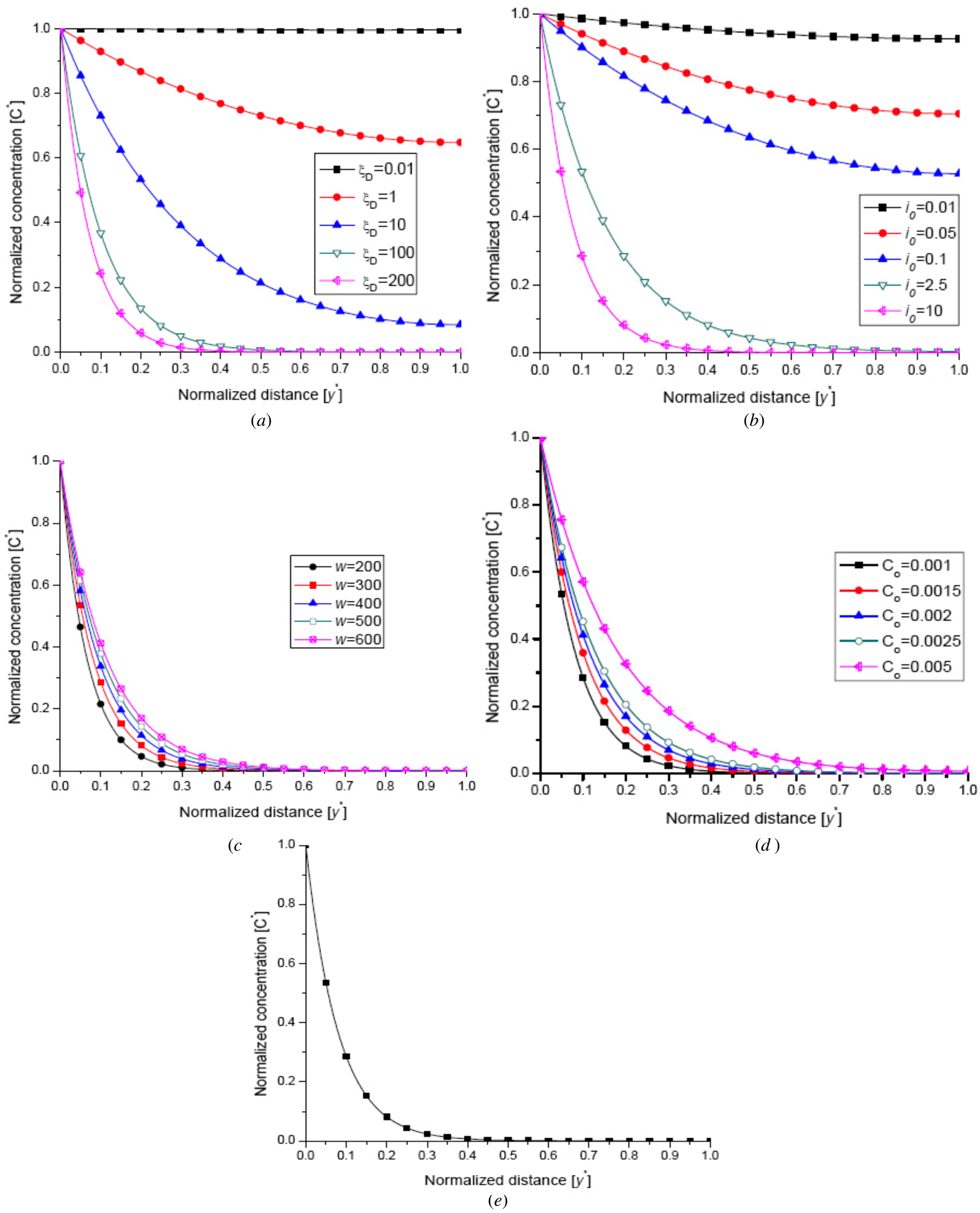

Figure 4. Concentration variation versus distance from the mouth of the channel as a function of (*a*) the nondimensional diffusion parameter, (*b*) current density, (*c*) channel height, (*d*) bulk concentration of Cu ions and (*e*) the real system.

the analysis demonstrates that realistically achievable height variations only slightly affect the diffusion changes possible in this particular system. The next variable considered is the bulk concentration of Cu ions. For the calculation, the 10 mA cm^{-2} current density and 300 μm height channel structure are selected. Four reasonable values of Cu ion concentration, bounded by solubility limitations, are chosen as 0.001 [1 M $CuSO_4$], 0.0015, 0.002, 0.0025 and 0.005 g mol cm^{-3}. Figure 4(*d*) shows the dependence of Cu ion depletion as a function of bulk Cu ion concentration. The figure shows that the diffusion of Cu ions can be improved by increasing the bulk concentration of Cu ions. However, ultimate limits on Cu ion concentration are given by solubility, and it will not be possible to have high enough concentrations of Cu ion to overcome the diffusion limitation. From these three analyses, it is possible to overcome electroplating bonding diffusion limitations; however, for a realistic system, the parameter changes required are not feasible. To consider

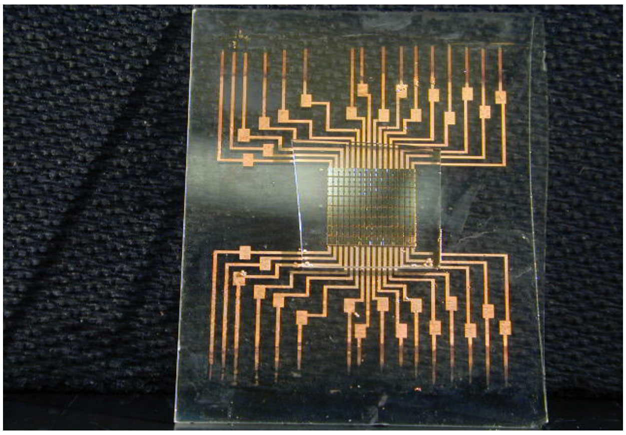

Figure 5. The electroplating bonded system in a diffusion environment.

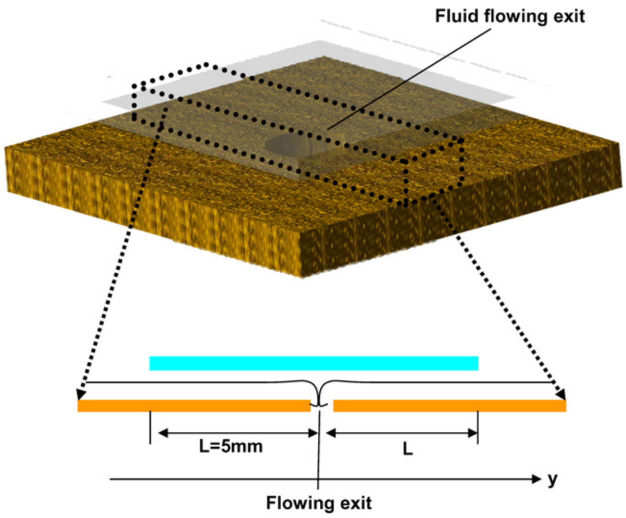

Figure 6. Schematic of a mass transfer system for a convective-diffusion model.

a more realistic system, the diffusion parameter for the experiment of the tested electroplating bonding system is calculated as $\xi_D = 157$**,** where C_0 is the bulk concentration of the Cu ions = 0.001 g mol cm^{-3}, the current density is $i_0 = 10$ mA cm^{-2} and the height of the channel is 300 μm. Figure 4(*e*) describes the relationship between normalized concentration and normalized distance.

The concentration of Cu ions falls to half the bulk value at a normalized distance of 0.05 and appears completely depleted at a normalized distance of 0.5 (in the real system, a distance of 0.25 cm). As mentioned above, realistic parameter changes are insufficient to solve this problem. New methods for either enhancing copper ion transport or changing the system configuration (for example, reduction in the number of interconnects) are required for successful electroplating bonding of realistic systems.

3.2. Experimental approach with diffusion

A Cu structure test-bed experiment was performed using a square array of 16 × 16 = 256 Cu posts, as shown in figure 5. The posts, which have 400 μm × 400 μm × 150 μm configuration and 16 electrical rows, were designed on a 1 cm × 1 cm area on both substrates. The fabrication was carried out using the general fabrication sequence described earlier. In this experiment, all of the electrical conduction lines were connected to get better electrical connectivity for electroplating purposes and selectively etched away with a Cu metal etchant after plating. This electroplating bonded metal post system passed the mechanical durability test described earlier. Then, the electrical continuity test was performed on the test rows with a multimeter. The measurement proved that the outmost test rows have electrical and mechanical continuity, but the test measurement on the inner test rows have shown electrical discontinuity. This failure phenomenon of a non-convective electroplating bonding system was predicted by the mass transfer theory described earlier. The theoretical calculations for the diffusion-environmental electroplating bonding system suggest that the electroplating bonding system requires a forced replenishment of the electroplating solution into the gap of the system. In order to achieve the external force for replenishment of the plating solution, convection of the electroplating solution which is a factor of mass transfer will be attempted to the system.

4. Electroplating bonding with a convection system

4.1. Theoretical approach for a flow channel system: convective-diffusion system

In electroplating on metal surfaces, agitation and circulation are recommended for obtaining uniform and smooth finishing. Both theoretical and experimental results for the diffusional system suggest that the electroplating solution inside the gap requires refreshment or circulation to enhance the electrodeposition of the ions. The relative importance of convection versus diffusion is represented by the Peclet number ($Pe = vL/D$), where v is a characteristic velocity in the channel, L is a characteristic dimension and D is the diffusivity of the species of interest. If $Pe \geqslant 1$, then convection plays an important role in the transport of Cu ion into the channel. If $Pe \ll 1$, convection is negligible and diffusion is the dominant transport mechanism [17].

For theoretical modeling of a convective-diffusion system, the assumptions of the diffusion modeling are maintained. As mentioned in the diffusion theory, the electrodeposition of the species of interest is dependent on the concentration of the species, and the concentration of the bulk electroplating solution is assumed constant during electrodeposition. The theoretical modeling is simplified by a channel formed by two substrates and a fluid flowing exit, as shown in figure 6. The boundary condition of ion concentration at the mouth of the channel being equal to the bulk concentration is maintained. Further, from the symmetry of fluid flow in the channel, it can be assumed that the derivative of the concentration of Cu ions at the center of the substrate with respect to position is equal to zero (i.e. $dC/dy = 0$ at the center of the channel).

Neglecting the electric field (drift) effect, but including both convection and diffusion, the flux of ions is given by [14]

$$J_{\mathrm{i}}(y) = -D_{\mathrm{i}}\frac{\mathrm{d}C_{\mathrm{i}}(y)}{\mathrm{d}y} + C_{\mathrm{i}}\upsilon_y, \tag{11}$$

where υ_y is the velocity (cm s^{-1}) with which a volume element in a solution moves along the axis. Applying conservation of mass to equation (11), the convective-diffusion equation of the electroplating bonding system can be expressed as

$$\frac{\mathrm{d}^2C_{\mathrm{i}}(y)}{\mathrm{d}y^2} - \frac{\upsilon_y}{D_{\mathrm{i}}}\frac{\mathrm{d}C_{\mathrm{i}}(y)}{\mathrm{d}y} = \frac{2i_0}{wnFC_0D_{\mathrm{i}}}C_{\mathrm{i}}(y), \tag{12}$$

where υ_y is the velocity of the convective fluid. To scale the system, as before,$C^* = C_{\mathrm{i}}(y)/C_0$ and $y^* = y/L$. Equation (12) can then be written in the nondimensionalized manner:

$$\frac{\mathrm{d}^2C_{\mathrm{i}}^*(y^*)}{\mathrm{d}y^{*2}} - Pe\frac{\mathrm{d}C_{\mathrm{i}}^*(y^*)}{\mathrm{d}y^*} - \xi_{\mathrm{D}}C_{\mathrm{i}}^*(y^*) = 0, \tag{13}$$

where $Pe(=\upsilon_yL/D_{\mathrm{i}})$ is the Peclet number based on the channel length and ξ_{D} is the diffusion parameter as described earlier. Boundary conditions are $C_{\mathrm{i}}^* = 1$ at $y* = 0$ and $\mathrm{d}C_{\mathrm{i}}/\mathrm{d}y^* = 0$ at $y* = 1$. Equation (13) is a homogeneous second-order linear differential equation with real constant coefficients. From the boundary conditions and general solution of equation (13),

$$C_{\mathrm{i}}^* = \frac{-\lambda_2\,\mathrm{e}^{\lambda_2}}{\lambda_1\,\mathrm{e}^{\lambda_1} - \lambda_2\,\mathrm{e}^{\lambda_2}}\,\mathrm{e}^{\lambda_1y^*} + \frac{\lambda_1\,\mathrm{e}^{\lambda_1}}{\lambda_1\,\mathrm{e}^{\lambda_1} - \lambda_2\,\mathrm{e}^{\lambda_2}}\,\mathrm{e}^{\lambda_2y^*}, \tag{14}$$

where $\lambda_1 = (Pe+\sqrt{Pe^2+4\beta})/2$, $\lambda_2 = (Pe-\sqrt{Pe^2+4\beta})/2$ and $\beta = \xi_{\mathrm{D}}$.

With geometry and plating solution parameters of the electroplating bonding system utilized in previous experiments, i.e. a diffusion parameter of 157, the concentration variation of Cu ions in the channel as parameterized by the Peclet number is described in figure 7(*a*) which is plotted by MATLAB 6.5 with calculation of equation (14). Figure 7(*a*) shows that the concentration of Cu ions in the channel increases as the Peclet number is increased. When the graph is obtained with a numerical analysis program, a threshold Peclet number which would provide a nearly uniform concentration of Cu ions in the microchannel approximating the bulk electroplating bath is expected. However, the numerical routine as originally programmed has a limitation for calculating concentration based on large *Pe*. So, a simplification of equation (14) for this case is performed by assuming that the convection term is dominant in the convective-diffusion equation, i.e. *Pe* has a very large value. In the assumption, the first term in equation (14) goes to zero and the constant term in the second term goes to unity. Therefore, equation (14) can be approximated for large *Pe* as

$$C_{\mathrm{i}}^* = \mathrm{e}^{\lambda_2y^*}. \tag{15}$$

The obtained equation is graphed to compare the calculation result to figure 7(*a*). Figure 7(*b*) shows a graph developed with equation (15). The graph in figure 7(*b*) shows almost the same tendency as the graph in figure 7(*a*).

With equation (15), a Peclet number analysis is performed to find a threshold Peclet number for acceptable system operation. Above the number, convection of the electroplating solution can introduce a plating solution which has a Cu ion concentration approaching that of the bulk solution. Approximately, we can define this threshold as a normalized concentration value of 0.9 over the entire normalized distance. To find this value, a numerical calculation is performed and the result is graphed in figure 7(*c*). The graph shows that the minimum Peclet number for obtaining sufficiently high concentration of the Cu ion in the channel is 1500. From this Peclet number, the minimum required velocity of a plating solution in the channel can be obtained. From the definition of the Peclet number,

$$Pe = \frac{\upsilon_yL}{D_{\mathrm{i}}}, \tag{16}$$

where υ_y is the fluidic velocity (cm s^{-1}), L is the channel length and D_{i} is diffusivity of the Cu ion (5.5×10^{-6} cm^2 s^{-1}). From equation (16), the minimum fluidic velocity can be calculated as 0.0165 cm s^{-1}. For a realistic cross-sectional geometry of channel, this results in a required volumetric flow rate of 0.11 ml min^{-1}. In the real experiment of the electroplating bonding system to be discussed in the following section, a mechanical pump circulated a plating solution with a nominal 20 ml min^{-1} = 3 cm s^{-1} velocity of solution. With this velocity, the Peclet number of the system to be tested can be obtained as

$$Pe = \frac{3\,\mathrm{cm\,s^{-1}} \times 0.5\,\mathrm{cm}}{5.5 \times 10^{-6}\,\mathrm{cm^2\,s^{-1}}} = 300\,000. \tag{17}$$

The reason for choosing such a high Peclet number is to consider the geometry of the entire electroplating bonding interconnect system (including dense arrays of interconnects) and to ensure success even though relatively large pressure drops through the narrow channel may lower the nominal velocity of the pump. Under these nominal conditions, figure 7(*d*) shows the predicted concentration variation with a normalized distance for the real experiments to be discussed in the following section. From the theoretical review of the convective-diffusion system, fluidic convection can improve the concentration of Cu ion through the channel.

4.2. Experimental approach for a flow channel system

The theoretical review of the conductive-diffusion effect in a microchannel system shows that forced convection of a plating solution can improve the concentration distribution of Cu ions in the channel. For maximum effectiveness, the proposed convective-diffusion electroplating bonding system requires a uniform convection effect on the entire system. To achieve this goal, a hole is drilled as a flow outlet for the forced-convective plating solution in the center of the bottom printed wiring board (PWB). The hole is 1 mm in a diameter. Then, a nipple is fitted to the hole using adhesive. The nipple is connected to an acid-resistant flow tube (MasterFlex precision tubing, Cole Parmer). This tube is selected for the plating solution convection because a copper electroplating solution usually includes sulfuric acid (H_2SO_4) for improving solution conductivity. By connecting the flow tube with a pumping system (MasterFlex, Cole Parmer), the convection rate of the

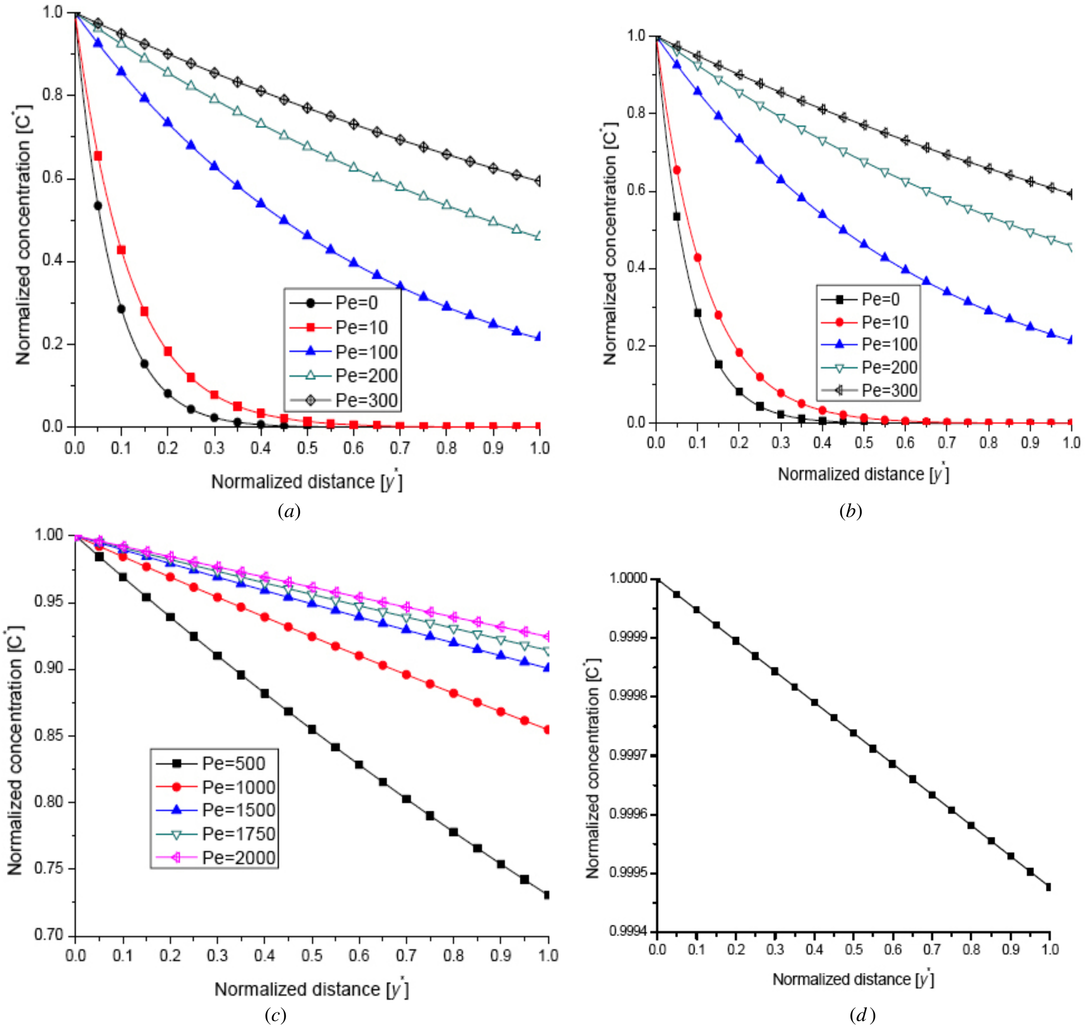

Figure 7. Concentration variation versus distance from the mouth of the channel as a function of (*a*) the Peclet number of equation (14), (*b*) the Peclet number of equation (15), (*c*) the Peclet number of variable fluidic velocity and (*d*) the Peclet number of the real system.

plating solution is controlled. The pump acts to suck fluid from the bulk plating solution through the microchannel and out of the hole/tube assembly. The pump output is returned to the bulk plating solution bath. That is, the convective plating solution system also creates a circulation of the plating solution. Figure 8 shows the convective-diffusion system for an electroplating bonding experiment.

A bottom PWB and a top glass substrate were utilized for the convective-diffusion electroplating bonding experiment. $16 \times 16 = 256$ posts were fabricated with the same fabrication procedure as the previous experiment. An etching protection layer that was formed by an extra SU-8 process analogous to a conventional passivation layer of the silicon chip and a metal layer was designed for preventing PWB etching during the RIE polymer mold etching step. After completion of the electroplating bonding, the mechanical integrity of the fabricated system was tested by the nitrogen flow-gun method described in section 2.3. Despite the evidence of mechanical connection between the two substrates, the system did not pass the electrical continuity test of resistance for the daisy-chain structures. In order to inspect the quality of the top substrate post to bottom substrate post bonding, the two substrates were separated by force. Figure 9 shows the separated substrates. The shiny surface of the bottom substrate shows that the PWB substrate is protected from RIE etching by the designed etch-stop layer. Figure 9(*a*) shows that approximately 70 posts are not electroplating bonded. However, the figure also shows that several posts around the center of the substrate have disappeared during the forced separation of the two substrates. This indicates that, in this central area, post-to-post mechanical connection was achieved by electroplating bonding. Therefore, it can be inferred that the concentration of Cu ions is high enough for effective electrodeposition to have occurred in this region. The reason for the electrical discontinuity of the connection line is illustrated in figure 9(*b*). The interconnects or posts on the bottom substrate are encompassed by polymeric material. The unexpected polymeric material has proven to be photoresist by inspection. For electroplating bonding of metallic structures, a photoresist layer is required for covering a seed layer on each of the

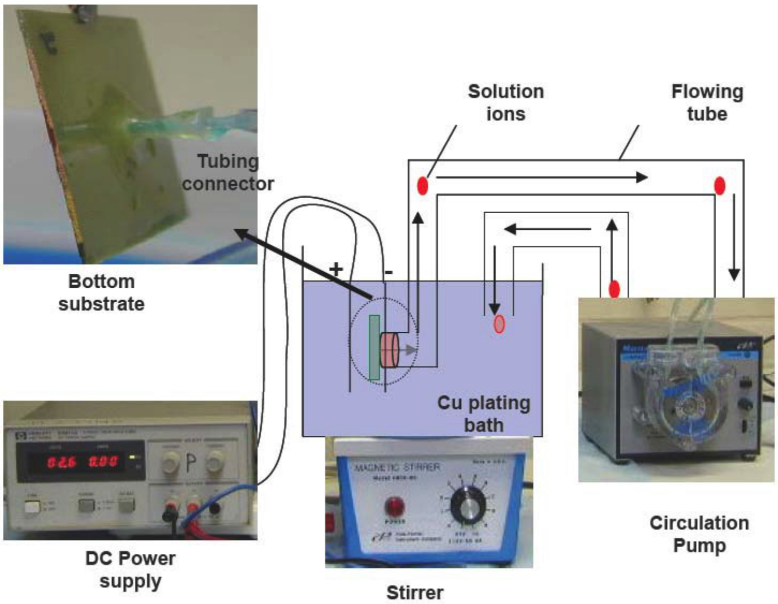

Figure 8. Photographs of an electroplating bonding system with convection.

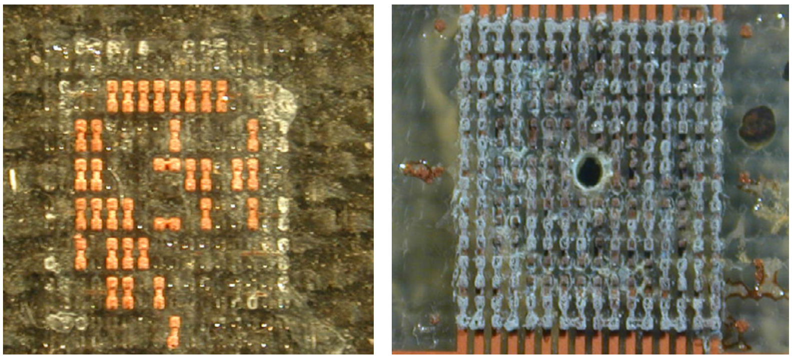

(*a*) (*b*)

Figure 9. Photographs of mechanically separated substrates. (*a*) Top substrate and (*b*) bottom substrate.

bottom and top substrates. Also, in this experiment, heat was also applied to improve the conductivity of the solution. The applied heat seems to help the contamination of the plating solution with a photoresist. This contamination may have prevented electrodeposition from occurring on some of the posts and, thereby, result in bonding failure of these posts.

5. Electroplating bonded chip interconnect system

From the previous experiments, the possibility of electroplating bonding was demonstrated. It also demonstrated that the plating solution flow channel system improved the electroplating bonding of the structures. Figure 10 shows an SEM picture of the electroplating bonding part of the structure that passed the mechanical test. From the picture, we know that the electroplating bonded structure yields a robust metal figure after electroplating. Figure 11 shows electroplating bonded structures detached from a

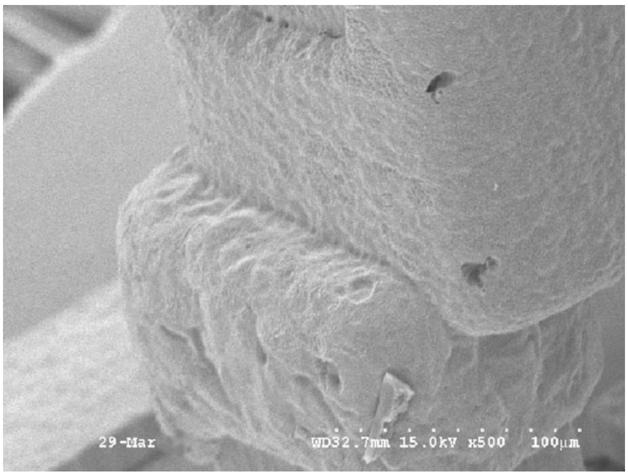

Figure 10. SEM picture of an electroplating bonded part of the interconnect.

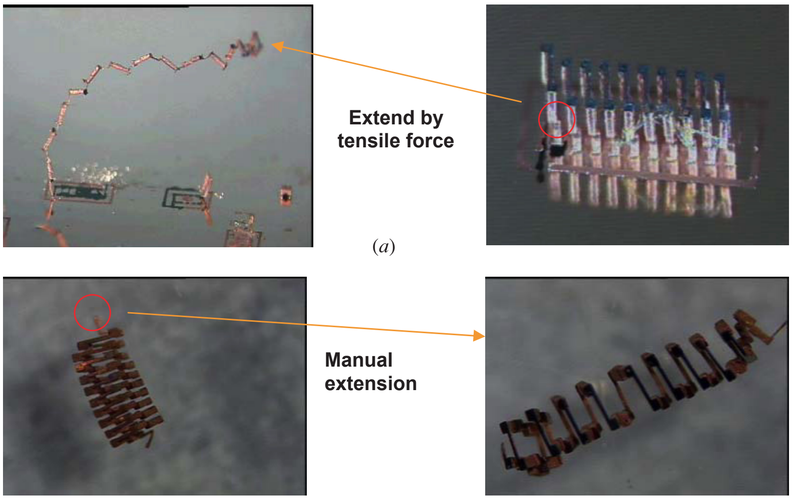

(*a*)

(*b*)

Figure 11. Photomicrographs of electroplating bonded structures undergoing a simple mechanical test. (*a*) Mechanical extension test of a ten-turn inductor and (*b*) spring-like inductor.

substrate. As in the figure, the electroplating bonded structures display substantial mechanical strength. Fabricated multi-bonded and multi-turn inductor structures [18] used as mechanical test structures are resistant to breakage and act like springs on a macroscopic level when large tensile forces are applied.

5.1. Design

The electroplating bonding technology is applied in the transformation of two Cu posts on separate substrates into a single, robust Cu structure. With the positive mechanical properties of the electroplating bonding structures confirmed, a chip interconnect test structure (glass to PWB) was designed and fabricated. In this work, glass was utilized instead of silicon chips for the convenience of substrate alignment. However, the design and fabrication approach would be the same for the chip. The primary goal of the design is to obtain Cu chip interconnects in the gap between the two substrates using the electroplating bonding method. For this sample, heat was not applied to the plating solution. This was done to minimize the degree to which the photoresist could have contaminated the plating bath. Otherwise, all other experimental conditions were the same as described above. Figure 12 shows photomicrographs of the fabricated electroplating bonding chip interconnect.

5.2. Result and discussion

The electrical characteristics of the chip interconnects were tested using the four-probe method. Measurement was executed with two test coupons. Each test coupon had 16 test rows. 14 test rows of test coupon A had good electrical continuity and test coupon B had 13 good test rows. The average electrical resistance of the chip interconnect test bed showed 0.097 Ohm/test row. The values agree well with the calculated electrical resistances of 0.092 Ohm/test row.

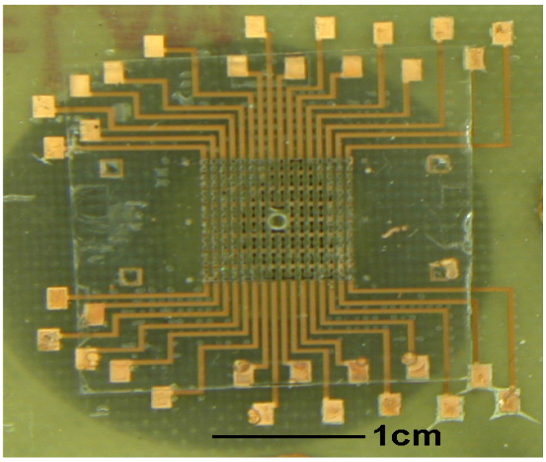

(*a*)

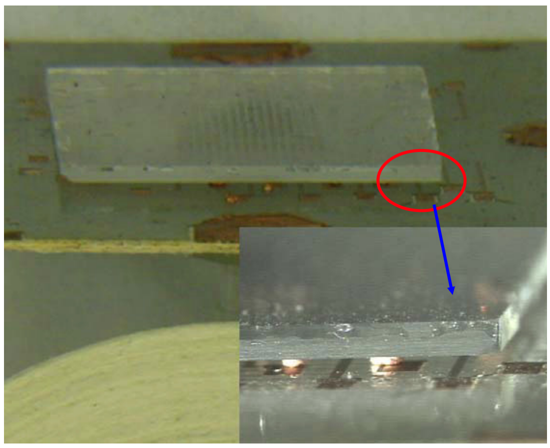

(*b*)

Figure 12. Photomicrographs of the fabricated electroplating bonded chip interconnect. (*a*) Top view and (*b*) side view.

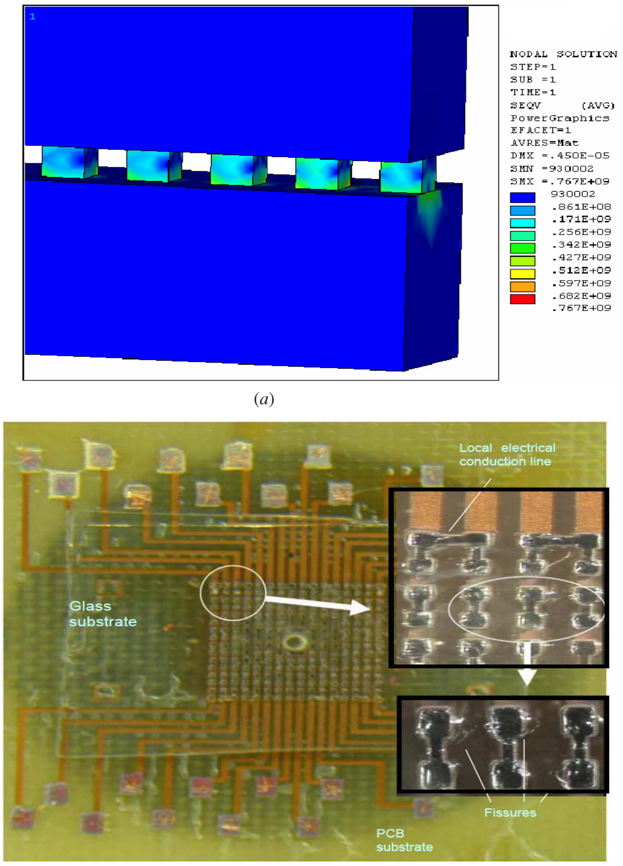

Figure 13. Photographs of (*a*) thermal-mechanical FEM simulation and (*b*) the chip interconnect system after thermal reliability test.

The temperature displacement of the system can be expressed by equation (18) [19]:

$$\delta = \Delta T(\alpha_{\mathrm{PWB}} - \alpha_{\mathrm{glass}})L, \qquad (18)$$

where δ is the difference between the thermally induced radial displacements of the PWB and the glass, α_{PWB} and α_{glass} are coefficients of thermal expansion in the PWB and glass substrates, respectively, and ΔT is the temperature change of the system (i.e. difference between the operating temperature and reference temperature). In this case, the reference temperature can be set as room temperature or as initial temperature of operation, and L is the radial distance from the center of the system. If the system is 1 cm × 1 cm, with a 100 °C temperature change, and typical values of $\alpha_{\mathrm{PWB}} =$ 20 ppm °C^{-1} and $\alpha_{\mathrm{glass}} = 2.8$ ppm °C^{-1} are utilized, then the mismatch of horizontal expansion in the system will be 12.2 μm. This mismatch will lead to stress on the system, especially at the interface between glass and Cu structures. A simple thermal-mechanical simulation using the finite element method (FEM) program ANSYS 8.0 showed that the interface of the adhesion layer between the interconnects and the seed layer had high stresses as shown in figure 13(*a*). This high-stressed profile around the interfacial layer was confirmed by reliability testing. The reliability tests were performed in a thermal chamber with a cycle range of −55 ~ +125 °C with a 5 min dwell at –55 °C and +125 °C and a 1 min transition time. The thermal test was cycled 100 times using the thermal chamber setup. After the thermal test, the electrical properties of the test coupons were again measured with the same result as the aforementioned electrical resistance data. Figure 13(*b*) shows the system after the reliability test. Many glass fissures can be seen on the top glass substrate. These were caused by thermal shock which occurred due to thermal mismatch between the glass and the PWB. This type of thermal failure can be solved by application of electroplating bonding to form interconnects that can undergo horizontal movement with minimal induction of stress during thermal cycling [20].

6. Conclusion

A bonding technology for establishment of substrate-spanning posts or structures is introduced in this paper. Theoretical and experimental approaches were applied to a diffusional and convective system. A single chip interconnect system was fabricated with 256 Cu interconnects based on the technology. The electroplating bonded structures demonstrated good electrical connectivity and mechanical strength. Convection during electroplating bonding was necessary to achieve mechanically stable and electrically continuous structures between two previously separate substrates. The minimum Peclet number for a good convective-diffusion electroplating bonding system was estimated to be 1500. For the given channel parameters, this corresponds to a fluidic volumetric velocity of 0.11 ml min^{-1}. The requirement of the flow channel for the electroplating bonding could cause difficulty in the assembly of the bonding system in the real world of IC or MEMS manufacturing. This can be solved by further theoretical study, similar to the approach of this work, of the physical processes that occur during electroplating bonding and by reviewing previous work related to electrodeposition of high aspect ratio trenches or vias. The relatively low velocity requirement suggests that several alternate, potentially more manufacturable, methods to flow the plating solution into the channel may be of interest. Such methods include gas sparging, panel movement and jet impingement [21]. Under these conditions, even if flow is not as effectively maintained as under the demonstrated convective flow system of this study, variation of current density, bath composition and system geometry [22, 23] can be considered to achieve similar results.

References

[1] Rusu C, Persson K, Ottosson B and Billger D 2006 LTCC interconnects in microsystems *J. Micromech. Microeng.* **16** S13–8

[2] Joo J and Choa S 2007 Deformation behavior of MEMS gyroscope sensor package subjected to temperature change *IEEE Trans. Compon. Packag. Technol.* **30** 346–54

[3] Tanaka S, Fujimoto S, Ito O, Choe S and Esashi M 2007 Laterally stacked glass substrates with high density electrical feedthroughs *J. Micromech. Microeng.* **17** 597–602

[4] Chu K, Choi W, Ko Y, Lee J, Park H and Jeon D 2007 Flip-chip bonding of MEMS scanner for laser display using electroplated AuSn solder bump *IEEE Trans. Adv. Packag.* **30** 27–33

[5] Lubecke V, Pardo F and Lifton V 2007 Polymer spacers for flip-chip optical MEMS *J. Microelectromech. Syst.* **16** 959–68

[6] Cabruja E, Collado A, Plaza J and Esteve J 2005 Piezoresistive accelerometers for MCM-package: II. The packaging *J. Microelectromech. Syst.* **16** 806–11

[7] Lin Y, Peng C and Chiang K 2002 Parametric design and reliability analysis of wire interconnect technology wafer level packaging *J. Electron. Packag.* **124** 234–9

[8] Joung Y and Allen M 2007 Chip-to-board micromachining for interconnect layer passive components *IEEE Trans. Compon. Packag. Technol.* **30** 15–23

[9] Pan L and Lin L 2001 Batch transfer of LIGA microstructures by selective electroplating and bonding *J. Microelctromech. Syst.* **10** 25–32

[10] Oh K and Ahn C 1998 Flip-chip packaging with micromachined conductive polymer bumps adhesive joining and coating technology in electronics manufacturing *Proc. 3rd Int. Conf. on Adhesive Joining and Coating Technology in Electronics Manufacturing* pp 224–8

[11] Burkett S, Temple D, Stoner B, Craigie C, Qiao X and McGuire G 2001 Processing techniques for vertical interconnects *Int. Symp. Semiconductor Device Research* pp 403–6

[12] Carano M 1986 Acid copper plating of high aspect ratio MLBs *Print. Circuit Fabr.* (December) 34–47

[13] Amadi S 1987 Plating high aspect ratio multilayer boards *Print. Circuit Fabr.* (October) 85–94

[14] Bard A and Faulkner L 1980 *Electrochemical Methods* (New York: Wiley)

[15] Jorne J and Tran A 2001 Additive-free electroplating of copper in high-aspect-ratio trenches *Proc. IEEE 2001 Interconnect Technology Conf.* 27–9

[16] Pesco A and Cheh H 1989 The current distribution within plated- through-holes *J. Electrochem. Soc.* **136** 399–407

[17] Takahashi K and Gross M 1999 Transport phenomena that control electroplated copper filling of submicron vias and trenches *J. Electrochem. Soc.* **146** 4499–503

[18] Joung Y, Nuttinck S, Yoon S, Allen M and Laskar J 2002 Integrated inductors in the chip-to-board interconnect layer fabricated using solderless electroplating bonding *2002 IEEE MTT-S Int. Microwave Symp. Digest* pp 1409–12

[19] Gere J and Timoshenko S 1997 *Mechanics of Materials* (Boston, MA: PWS Publishing)

[20] Joung Y 2003 Electroplating bonding technology for chip interconnect, wafer level packaging and interconnect layer structures *PhD Thesis* Georgia Institute of Technology, Atlanta

[21] Hazlebeck D and Talbot J 1999 Modeling of the electroplating of a through-hole considering additive effects and convection *J. Electrochem. Soc.* **138** 1985–97

[22] Mikkola R and Chen L 2000 Investigation of the roles of the additive components for second generation copper electroplating chemistries used for advanced interconnect metallization *Proc. IEEE 2000 Interconnect Technology Conf.* pp 117–9

[23] Hoshino K, Yagi H and Tsuchikawa H 1990 Effect of titanium addition to copper interconnect on electromigration open circuit failure *Proc. 1990 7th Int. IEEE VLSI Multilevel Interconnection Conf.* pp 357–9